AXISYMMETRIC AND THREE-DIMENSIONAL FLOW SIMULATION OF A MIXED COMPRESSION SUPERSONIC AIR INTAKE

Soltani M.R.,* Abedi M.,§ Askari R.,† and Sepahi Younsi J.♦
*Author for correspondence
Aerospace Engineering Department,
Sharif University of Technology,
Tehran, Iran,
E-mail: msoltani@sharif.edu

ABSTRACT

The flow of an axisymmetric supersonic mixed compression air intake has been simulated numerically in order to investigate the effects and also the necessity of three-dimensional (3D) modeling. For this purpose, the supersonic intake has been simulated numerically via axisymmetric and 3D CFD solver, solving steady state Reynolds-averaged Navier-Stokes equations along with SST k-ω turbulence model, at free-stream Mach number of 2.0 at zero angle of attack. The grid of the 3D cases was a 14.4-degree sector, instead of a 360-degree domain, with rotational periodic boundary condition for side boundaries. The results show that the static and total pressure distribution almost matches well with experimental data for both the axisymmetric and 3D simulations. If the prediction of performance parameters is the main goal of simulations, it seems that axisymmetric simulation presents adequate accuracy and 3D simulation is not a reasonable choice. 3D numerical simulation results in a more detailed study on supersonic intakes, including shock-boundary layer interaction, the location of terminal shock, and consequent separation point. 3D effects in axisymmetric supersonic intakes in axisymmetric flow condition are not enough strong to affect significantly on the intake performance in all operational condition. However, it seems that these effects play a more important role in critical and weak supercritical condition at steady state operation.

NOMENCLATURE

AP	[-]	Axisymmetric plane
FD	[-]	Flow distortion
M	[-]	Flow Mach number
MFR	[-]	Intake mass flow ratio
P	[Pascal]	Flow pressure
SBLI	[-]	Shock-boundary layer interaction
TPR	[-]	Intake total pressure recovery

Special characters

$\Delta_{3D\ to\ Ax}$	[%]	The difference of 3D and axisymmetric value over the axisymmetric value
ϕ	[degree]	Degree around axis

Subscripts

e	End section of intake
o	Stagnation point condition
s	Static condition
∞	Free stream condition

*Professor, §M.Sc. Graduate, and †Ph.D. Student, Aerospace Engineering Department, Sharif University of Technology, Tehran, Iran.
♦Assistant Professor, Mechanical Engineering Department, Ferdowsi University of Mashhad, Mashhad, Iran.

INTRODUCTION

Air intakes play an important role in the stability and performance of the installed propulsion systems and as a result in overall flying vehicle operation. In this subject, supersonic air intakes have a crucial role, since they must meet the need of the engine for sufficient air with qualified characteristics, such as low pressure-loss and distortion, in all flight conditions, running from stationary operation to supersonic flight [1]. Furthermore, supersonic intakes have complex flow-field involving several shocks and expansion waves, shock-boundary layer interaction (SBLI), separation, buzz instability, etc.; therefore, experimental and numerical analysis of them are necessary to understand the flow-field and predict operation characteristics and intake behavior on design and off-design points. There are several classifications for supersonic intakes based on their characteristics, like geometry or compression mechanism. The two-dimensional (2D) and axisymmetric CFD analysis of intakes are conventional respectively for rectangular and axisymmetric/semi-axisymmetric intake, which neglect the 3D effects of flow-field. However, 3D effects, for example due to sidewall and cross flows, particularly in separation and shock-boundary layer interaction regions for all air intake types, are considerable [2, 3]. Loth et al. conducted a series of 2D numerical analysis using k-ε turbulence model on a ramped intake at M=2.0 [4]. Ran and Mavris performed a 2D CFD simulation to test and verify their design method for 2D mixed-compression intake [5]. Mizukami and Saunders ran a 2D Navier-Stokes solver on a rectangular mixed-compression intake and compared the results of various grids and turbulence models with experimental data [6]. Chang et al. used an unsteady 2D code with SST k-ω turbulence model to simulate a hypersonic inlet flow [7]. Bourdeau at al. performed a 3D numerical simulation with k-ε turbulence model to verify their high-speed intake design method [8]. Aziz et al. ran a time-dependent RANS 3D code on a structured grid of a supersonic intake's computational domain [9]. Terappier et al. conducted an unsteady 3D CFD solver using DDES on a mixed-compression intake and compared their result with experimental data [10, 11]. Although 3D CFD analysis provides more accuracy, it needs more CPU time, and it is a basic question if it is necessary or advantageous to run 3D CFD solver instead of 2D one – the question that has not been answered by all such mentioned studies.

To answer this question, a supersonic mixed-compression intake designed for free stream Mach number of 2.0 at zero angle of attack was chosen to simulate axisymmetric and three-dimensional to compare their results. The intake was beforehand tested experimentally in design and off-design operation points, various Mach numbers, angles of attack, and back-pressure by the author [12-18]. Figure 1 shows schematic of the intake model. Total pressure probes were located at Rake at $\phi=0^o$, and static pressure probes were located on the surface of the central body, called spike, at $\phi=0^o$ from compression ramp to the Rake position.

The more important parameters related to intake performance are Mass Flow Ratio (MFR), Total Pressure Recovery (TPR), and Flow Distortion (FD), that all of them are non-dimensional and between 0.0 and 1.0. MFR is the mass flow passing through intake duct over the maximum mass flow that can enter to the duct [12]. TPR is the average of total pressure at the exit cross-section of the intake (engine or combustion chamber entrance) divided by total pressure of the free stream [12], and FD represents the flow uniformity at the mentioned section that is the ratio of the maximum and minimum difference of the total pressure to its average. The upper values of MFR and TPR, and lower for FD are favorable. Figure 2 depicts the schematic of intake performance curve and its operating condition.

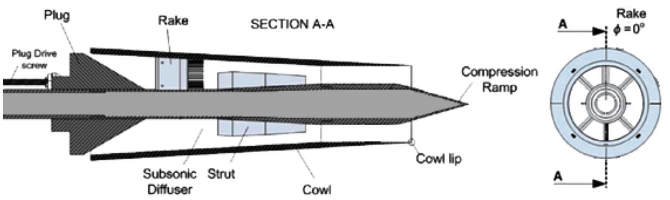

Figure 1 Schematic of the intake model

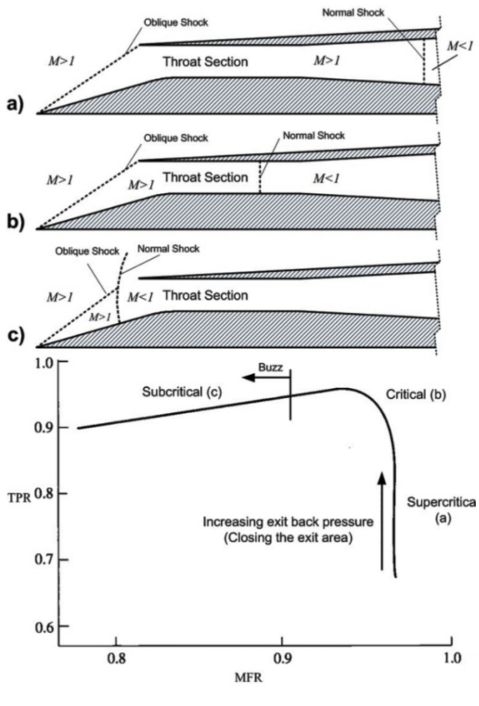

Figure 2 Supersonic intake performance curve and its operating conditions [17]

NUMERICAL SETUP

Figure 3 shows the axisymmetric grid and computational domain of the intake along with all of their boundary conditions. The steady state Reynolds Averaged Navier-Stokes equations in combination with SST k-ω turbulence model equations was solved by a density-based approach both axisymmetric and 3dimensionally on the computational domain presented here. The Courant number was 1.0, and the second-order upwind discretization was applied. Adiabatic no-slip wall boundary condition was considered for wall boundaries.

The structured grid was used for axisymmetric simulation containing almost 250,000 cells, and as it is shown in Figure 3, it was refined or stretched in all or part of the physical domain in order to capture physical phenomena and meet y-plus requisite for the turbulence model. Hereafter, this plane is named Axisymmetric Plan or AP. The grid of the 3D cases was generated by revolving the AP ($\phi=0^o$) around the axis by $\phi=\pm7.2^o$, and rotational-periodic boundary condition was set for side boundaries, Figure 4. Therefore, it was a 14.4-degree sector instead of a 360-degree of the physical domain containing almost 3,500,000 cells, and the 3D grid in any rotational plane was the same as the AP.

The simulation was conducted for a back-pressure related to a specific supercritical operation, $P_{s,e}/P_{s,\infty}=5.5$ as the based case, in order to compare its results with experimental data. Afterward, two other back-pressures upper and lower than the based case ($P_{s,e}/P_{s,\infty}=4.7$ and 5.9) simulated to study the difference between the 3D and axisymmetric simulations on intake performance. The more information about the mechanism of changing back-pressure in experimental tests is available in [12]. Other flow parameters for boundary condition were set based on the experimental wind tunnel experiments where M=2.00221 and Turbulence Intensity was 5%.

It should be considered that all of the numerical simulation presented here were conducted without modeling and simulation of four struts and Rake illustrated in Figure 1. Although they could affect the reality and accuracy of numerical simulations, since the flow 3D effects investigation and comparison between axisymmetric and 3D simulation are the main subjects of this paper, these details of geometry were ignored to have no effect on simulation results and their analysis.

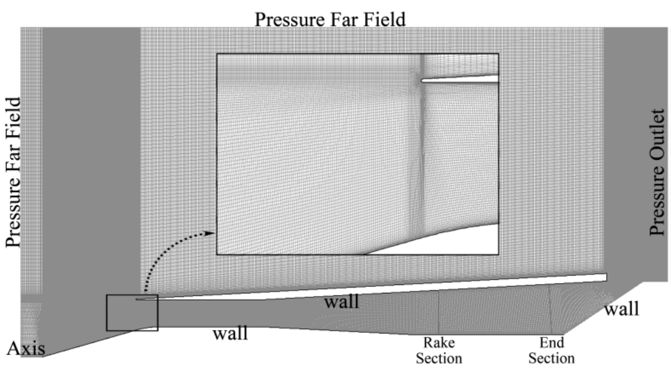

Figure 3 Axisymmetric Plane grid and details of boundary conditions

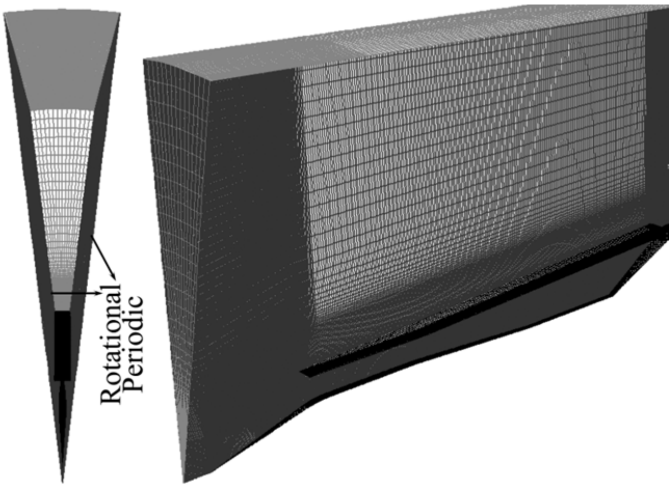

Figure 4 3D simulation computational domain and grid

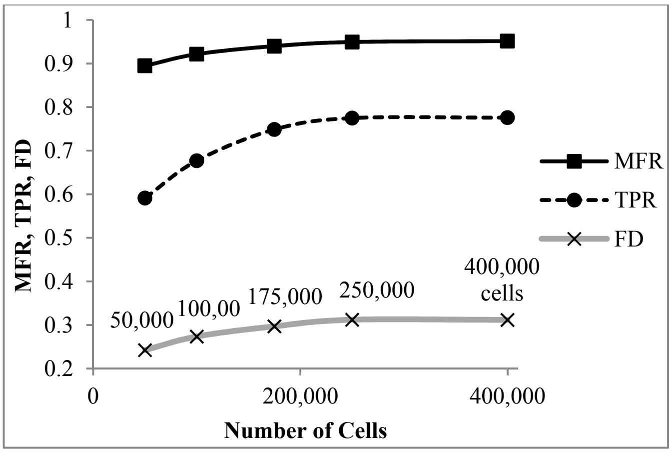

Figure 5 Results of grid-independency study on AP

RESULTS

Validation and verification

As mentioned, the AP and 3D structured grids had almost 250,000 and 3,500,000 cells respectively. The results of the grid independency study on finer and coarser grid resolution indicate that the current grids established the best balance between accuracy and CPU time, Figure 5. The convergence accuracy of flow parameters was 10e-4, and the y-plus near wall boundaries was 0.5 to 5 – almost y+≈1.

Figure 6 shows the distribution of static pressure ratio on the spike, and Figure 7 shows the distribution of total pressure ratio at the Rake section for axisymmetric, 3D simulation, and experimental data at $P_{s,e}/P_{s,\infty}$=5.5. At a glance, it is clear that there is not a significant difference between the axisymmetric and 3D simulations for the spike static pressure as well as the Rake total pressure. A good agreement between the values and trends of the static pressure along the spike for both simulations and experimental data from the nose to end is seen in Figure 6. It demonstrates that both the numerical simulations performed well to capture the strength and positions of external and internal shocks and expansion waves. The static pressure drops and jumps correspond to local expansion waves and internal oblique and terminal shocks shown in Figure 8.

Moreover, the numerical and experimental total pressure near the cowl are well matched as it is shown in Figure 7. The area-weighted average of total pressure for the simulations differs less than -1.12% from experimental results. However, this difference has more amount in core-flow and near the spike, that is -5.31% and 4.99% respectively. In order to investigate this differences in more details, the related local Mach number contours along with flow stream lines of axisymmetric simulation at $P_{s,e}/P_{s,\infty}$=5.5 is shown in Figure 9. As it is evident, there is not almost the region of separation in near the cowl, but there is a big one near the spike; as a result, the simulation errors (although are in small values) is corresponding to prediction of the flow in the regions including the flow SBLI and resulted in flow separations.

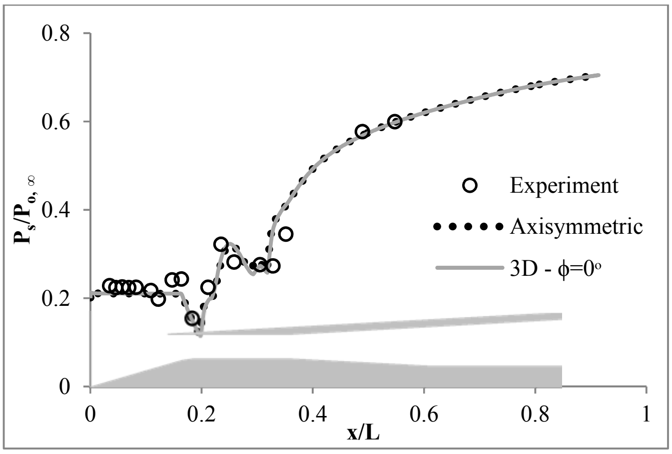

Figure 6 Distribution of the ratio of static pressure to free stream total pressure on the spike at $P_{s,e}/P_{s,\infty}$=5.5

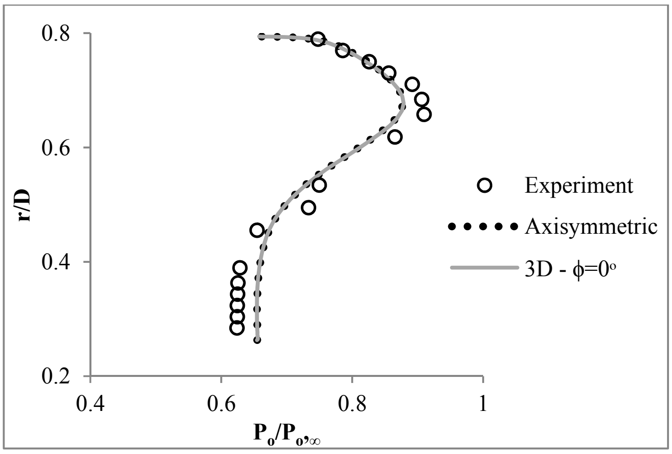

Figure 7 Distribution of the ratio of total pressure to free stream total pressure for Rake at $P_{s,e}/P_{s,\infty}$=5.5

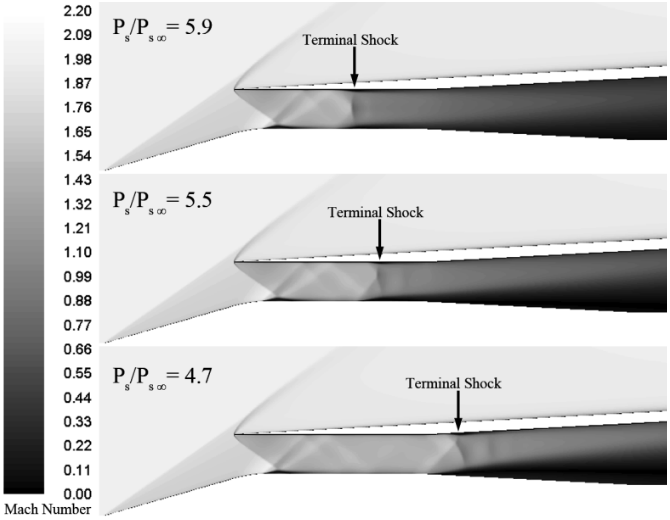

Figure 8 Contours of Mach number for axisymmetric simulation

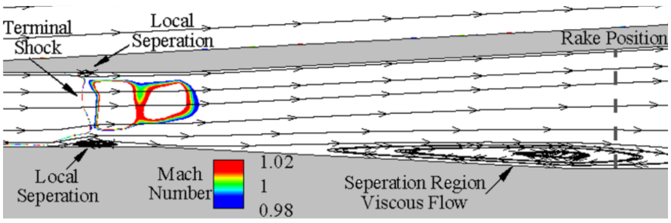

Figure 9 Streamline in diffuser at $P_{s,e}/P_{s,\infty}$=5.5

AP and 3D Comparison

The contours of Mach number for axisymmetric numerical simulation for various $P_{s,e}/P_{s,\infty}$ is shown in Figure 8, As it is seen in this figure, the increase in $P_{s,e}/P_{s,\infty}$ leads to change intake operational condition from supercritical to critical during which the internal terminal shock moves upstream from the diffuser toward throat and becomes weaker. This upstream movement and weakening of the terminal shock are responsible for the improvement of performance parameters like increase of TPR and decrease of FD at a constant MFR. The conical shock located at the spike nose and the flow spillage due to the distance between its direction and cowl-lip position control the MFR. Until the free stream Mach number is constant, MFR is constant as the back-pressure changes in critical and supercritical operation.

Values of the intake performance parameters and the percentages of their changes for 3D to axisymmetric simulations are written in Table 1, and not to mention that the performance parameters calculate at the end section of the diffuser shown in Figure 3. Table 1 expresses that the trends of variation in the performance parameters by changing in back-pressure are according to the expected behavior in both the axisymmetric and 3D simulations [12].

The difference of 3D and axisymmetric values over axisymmetric values is defined as $\Delta_{3D\ to\ Ax.}$. This parameter clarifies that the calculated performance parameters via both the axisymmetric and 3D simulations are consistent very well. The maximum changes in MFR, TPR, and FD are 0.10%, -0.05%, and -2.11% respectively, all of them for $P_{s,e}/P_{s,\infty}$=5.9 condition. These differences are very small and it cannot be fair that these account as the advantage of 3D simulation versus axisymmetric one. Therefore, if the prediction of performance parameters is the main goal of simulations, axisymmetric simulation present adequate accuracy, and 3D simulation is not a reasonable choice.

As mentioned, since the free stream Mach number is constant, MFR is constant in all simulated cases, which are at the critical and subcritical condition. MFR is 0.1% more for 3D simulation than axisymmetric simulation. It may be because of 3D effects that cause to reduce the conical shock angel and as a result reduce the gap between shock and cowl-lip; therefore, the flow spillage decreases and the MFR increases. It is seen from Table 1 that 3D simulations predict TPR a few less and FD a few more than axisymmetric simulations do; moreover, the values of changes increased as moving from supercritical to critical condition.

Figure 10 shows the distribution of shear stress on the spike surface for both the simulations. The sharp drop in wall shear stress value indicates the boundary layer separation point. As it is shown in Figure 10, the sharp drop in shear stress values located more upstream for axisymmetric cases than 3D ones, and this difference is bigger from supercritical to critical operation. It seems that 3D effects in viscous layer increase the flow momentum and make it more attached which causes that the separation points, particularly due to SBLI, occur later. This separation is shock-induced separation, and its position strongly depends on the terminal shock position and intake's diffuser geometry gradient. Hence, an accurate prediction of this separation point strongly depends on the accurate prediction of SBLI and specially terminating shock position. For the case of $P_{s,e}/P_{s,\infty}$=5.5 and 5.9, the terminal normal shock is located in the throat where there is no variation in geometry and shock position and strength are more important in the determination of separation point, so 3D effects could be more effective for these $P_{s,e}/P_{s,\infty}$ conditions. Moreover, since upstream terminal shocks are weaker than downstream ones, the terminal shocks and SBLI for critical operation are weaker than for supercritical condition; as a result, the 3D effects have more influence on them.

For $P_{s,e}/P_{s,\infty}$=4.7 condition, the terminal normal shock is located in the regions downstream of the throat, so it seems that the geometry gradient plays the main role in the determination of the shock position. In addition, it is the most supercritical condition presented here. Therefore, the terminal shock is stronger and SBLI is too strong to be affected by meager 3D effects. Hence, the shear stress and separation points do not differ between 3D and axisymmetric simulations at $P_{s,e}/P_{s,\infty}$=4.7.

Figure 11 shows the structure and position of the terminal shock at $P_{s,e}/P_{s,\infty}$=5.5 for the 3D and axisymmetric simulations. It reveals that the little change in separation points leads to change in normal shock position. Overall, considering the fact that the more downstream terminal shock, the stronger shock and SBLI and as a result more pressure loss, the 3D simulation calculate the TPR less than axisymmetric simulation does, and this difference is bigger in near critical condition.

Table 1 Intake performance parameters for axisymmetric and 3D, and the percentage of 3D to axisymmetric changes

	MFR			TPR			FD		
$P_{s,e}/P_{s,\infty}$	4.7	5.5	5.9	4.7	5.5	5.9	4.7	5.5	5.9
Axisymmetric	0.950	0.950	0.950	0.706	0.775	0.815	0.565	0.312	0.193
3D	0.951	0.951	0.951	0.705	0.774	0.814	0.564	0.310	0.189
$\Delta_{3D\ to\ Ax.}$ (%)	0.10	0.10	0.10	-0.02	-0.03	-0.05	-0.17	-0.56	-2.11

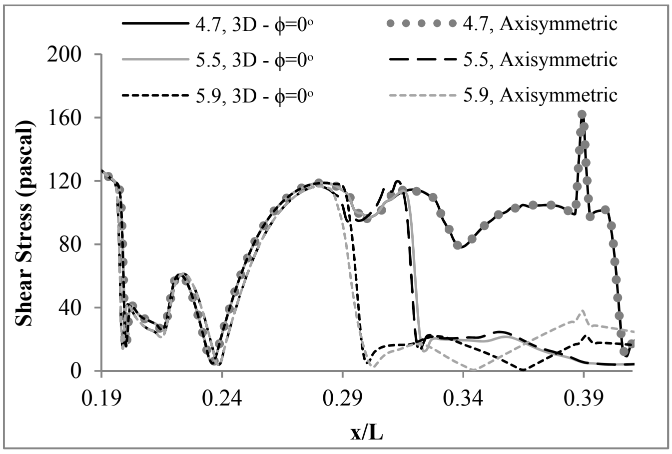

Figure 10 Distribution of shear stress on spike

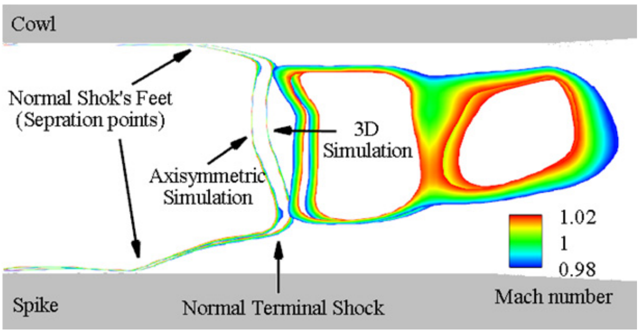

Figure 11 Position of terminal shock at $P_{s,e}/P_{s,\infty}$=5.5

Meanwhile, although the 3D effects are very small, they are more effective in flow with lower velocity. In this way, 3D effects in the subsonic flow in diffuser provide the flow with the opportunity to become uniform; therefore, FD increases. Since the subsonic region in diffuser increases by upstream movement of terminal shock, the change in FD increases as $P_{s,e}/P_{s,\infty}$ increases.

Finally, it deserves to mention that the main effect of 3D simulation that is tangential velocity component is less than 0.01% at any axial sections and rotational plans. Furthermore, the contours of Mach number in any rotational plans have not a differentiable difference from each other; therefore, they are the same as its contours on AP and the same as those for axisymmetric simulations shown in Figure 8.

Overall, when it comes to the absolute values of changes in such parameters as pressure, Mach number, MFR, TPR, and FD, it is concluded that 3D simulation in axisymmetric intake at zero angle of attack, which results in axisymmetric flow, has no considerable advantage on the stable intake operation in comparison with axisymmetric flow simulation. Since it seems that the effects of 3D simulation increased in the lower speed of flow and weaker shock waves and their interaction with boundary layer, it is probable that 3D effects play a more effective role in critical intake operation than supercritical operation. Therefore, it is probable that 3D simulation predicts flow with more accuracy related to flow unsteadiness phenomena such as terminating shock oscillations or especially subcritical intake instability, called BUZZ. However, this issue is not in the scope of this paper, because it needs to conduct wide unsteady simulations.

CONCLUSION

The 3D and axisymmetric numerical simulations of the supersonic mixed compression air intake at free stream Mach number of 2.0 at zero angel of attack are well-matched with experiment. The study of performance parameters of the intake asserts that even with the meticulous approach, the difference between results of the 3D and axisymmetric simulations is ignorable and has no considerable effects to predict the intake performance because the maximum difference in any cases is almost less than 0.5%. Therefore, the flow field in any rotational plans is almost the same as the axisymmetric one.

The 3D simulation has not any effects on the patterns of the flow field. Meanwhile, 3D effects play little role in the flow field with relatively lower velocity, especially subsonic regions in diffuser and separation regions due to shock-boundary layer interaction. 3D effects cause boundary layer becomes more attached and delays the separation points. Therefore, the terminal shock locates at the downstream in compare with axisymmetric simulation, so total pressure recovery declines.

As the back-pressure increase, upstream movements of terminal shock leads to occur subsonic region in more extent, which results in flow uniformity due to 3D effects. Thus, the flow distortion is calculated lower at bigger back-pressure for the 3D simulations in compare with the axisymmetric ones.

The increase in mass flow rate for the 3D simulations is probably because of the decrease in the conical shock angel that which results in the gap reduction between conical shock and cowl-lip. As a result, the flow spillage reduces, and MFR increases.

Finally, the axisymmetric simulations have enough accuracy for axisymmetric intake in stable axisymmetric flow, and the 3D simulation, which needs several times of CPU-time, provides no more accuracy and is not worth its cost. Therefore, the 3D simulation for axisymmetric intake in axisymmetric flow condition at stable operation is neither necessary nor advantageous.

REFERENCES

[1] Mattingly, J.D. and Von Ohain, H., Elements of Propulsion: Gas Turbines and Rockets, *American Institute of Aeronautics and Astronautics Reston*, USA, 2006

[2] Loth, E., et al., Canonical Normal Shock Wave/Boundary-Layer Interaction Flows Relevant to External Compression Inlets, *AIAA Journal*, Vol. 51, No. 9, 2013, pp. 2208-2217

[3] Fisher, S., Three-dimensional Flow Effects in a Two-Dimensional Supersonic Air Intake, *Journal of Propulsion and Power*, Vol. 2, No. 6, 1986, pp. 546-551

[4] Loth, E., et al., Mesoflap and Bleed Flow Control for a Mach 2 Inlet, *42nd AIAA Aerospace Sciences Meeting and Exhibit*, 2004

[5] Ran, H. and Mavris, D., Preliminary Design of a 2D Supersonic Inlet to Maximize Total Pressure Recovery, *AIAA 5th Aviation, Technology, Integration and Operations Conference*, 2005

[6] Mizukami, M. and Saunders, J., Parametrics on 2D Navier-Stokes Analysis of a Mach 2.68 Bifurcated Rectangular Mixed-Compression inlet, *31st Joint Propulsion Conference and Exhibit, Joint Propulsion Conferences*, 1995

[7] Chang, J., et al., Classifier Utility Modelling and Analysis of Hypersonic Inlet Start/Unstart Considering Training Data Costs, *Acta Astronautica*, Vol. 69, No. 9, 2011, pp. 841-847.

[8] Bourdeau, C., et al., Three-Dimensional Optimization of Supersonic Inlets, *AIAA Paper*, 1999, pp. 99-2108

[9] AZIZ, M., Elbanna, H., and Abdelrahman, M., Design Optimization of a Three Dimension Supersonic Intake Using the CFD-RC Package, *Tenth International Congress of Fluid Dynamics (ICFD10)*, 2010

[10] Trapier, S., Deck, S., and Duveau, P., Delayed Detached-Eddy Simulation of Supersonic Inlet Buzz, *AIAA Journal*, Vol. 46, No. 1, 2008, pp. 118-131

[11] Trapier, S., Duveau, P., and Deck, S., Experimental Study of Supersonic Inlet Buzz, *AIAA Journal*, Vol. 44, No. 10, 2006, pp. 2354-2365

[12] Soltani, M.R., Sepahi Younsi, J., and Daliri, A., Performance Investigation of a Supersonic Air Intake in The Presence of The Boundary Layer Suction, *Proceedings of the Institution of echanical Engineers, Part G: Journal of Aerospace Engineering*, Vol. 229, No. 8, 2015, pp. 1495-1509

[13] Soltani, M.R., Sepahi Younsi, J., and Farahani, M., Effects of Boundary-Layer Bleed Parameters on Supersonic Intake Performance, *Journal of Propulsion and Power*, Vol. 31, No. 3, 2015, pp. 826-836

[14] Soltani, M.R., Daliri, A., Sepahi Younsi, J., and Farahani, M., Effects of Bleed Position on the Stability of a Supersonic Inlet, *Journal of Propulsion and Power*, Vol. 32, No. 5, 2016, pp. 1153-1166

[15] Soltani, M.R., Abedi, M., and Sepahi Younsim J., Experimental Investigation of Instability of a Supersonic Mixed Compression Air Intake, *Modares Mechanical Engineering*, Vol. 15, No. 14, 2015, pp. 93-100 (In Persian)

[16] Soltani, M.R., Abedi, M., and Sepahi Younsim J., Experimental Investigation of the Buzz Cycle in a Supersonic Axisymmetric Intake, *Modares Mechanical Engineering*, Vol. 14, No. 16, 2015, pp. 311-320 (In Persian)

[17] Soltani, M.R., Sepahi Younsi, J., and Daliri, A., Performance Investigation of a Supersonic Air Intake in Presence of Boundary Layer Bleed, *32nd AIAA Applied Aerodynamics Conference*, 2014

[18] Soltani, M.R. and Sepahi Younsi, J., Buzz Cycle Description in an Axisymmetric Mixed-Compression Air Intake. *AIAA Journal*, Vol. 54, No. 3, 2015 pp. 1040-1053